IOSR Journal of Applied Chemistry (IOSR-JAC)
e-ISSN: 2278-5736.Volume 10, Issue 9 Ver. III (September. 2017), PP 55-64
www.iosrjournals.org

Nonenzymatic Sensing Of Methyl Parathion Based On RGO-Zno Nanocomposite Modified Glassy Carbon Electrode

S. Muthumariappan, C.Vedhi*
PG & Research Department of Chemistry, V.O Chidambaram College, Tuticorin –628008, Tamilnadu, India
Corresponding Author: C.Vedhi

Abstract: *A simple one-pot hydrothermal synthesis strategy has been approached to prepare the composite viz.reduced graphene oxide-ZnO nanoparticles (~30 nm)(RGO–ZnO).The synthesized RGO–ZnO composite has been successfully applied for glassy carbon electrode (GCE) surface modification. The RGO–ZnO composite-modified GCE is applied for sensitive and selective determination of Methyl Parathion(MP).The as-prepared composite is characterized by using Fourier Transform Infra-Red Spectroscopy(FT-IR),Scanning Electron Microscopy (SEM) along with Energy Dispersive X-ray (EDX) and elemental mapping. The atomic force microscopy (AFM) and Transmission electron microscope (TEM) with SAED analysis confirm the presence of ZnO nanoparticles embedded over the entire surface of reduced graphene oxide. The electrochemical behavior of Methyl parathion is performed by using cyclic voltammetry and Square wave Voltammetry methods. The chemical sensor exhibited a linear dependence on MP concentration ranging from 5 x10^{-9} to 100 x 10^{-9}M with a detection limit of 1.22 x 10^{-9} M (S/N = 3). The present method was applied to determining methyl parathion in real samples of vegetables. The sensors for methyl parathion exhibit high sensitivity and good reproducibility and are promising for fast, simple, and sensitive analysis of Organophosphate pesticides (Ops) in environmental and biological samples.*

Keywords*: Non enzymatic sensor, RGO-ZnO nano composite. Methyl parathion.*

Date of Submission: 26-09-2017 Date of acceptance: 07-10-2017

I. Introduction

Organophosphate pesticides (OPs) are a group of organic pesticides with high toxicity. They are widely used in agriculture as typical insecticides to enhance production and quality with a wide range of activity and are also used for chemical warfare. The residue of OPs in the natural environment generates lots of pollution problems because of their high toxicity [1, 2]. Therefore, it is essential to develop some convenient, sensitive and effective detection methods for OPs in food and environmental samples. The traditional methods to determine OPs are chromatography either using GC-MS [3] or high performance liquid chromatography [4,5]. On the other hand, biosensors based on the inhibition of acetylcholinesterase [6–8] and electrochemical sensors based on hydrolysis enzyme of Ops [9, 10] have been used for the determination of OPs in the environment. Nowadays, nonenzymatic electrochemical sensors have also been developed for the detection of Ops [11, 12]. These electrochemical methods not only simplify test process for OPs, but also improve the detection efficiency. Many OPs, such as methyl parathion (MP), belong to aromatic nitro compounds which easily undergo redox reaction. This feature is favorable for their direct electrochemical detection.

Reduced graphene oxide (RGO) is a promising material and recently it has drawn greater attention in various fields. RGO possess unique physicochemical properties like high surface area [13-15], easy to functionalize with other materials [16] and it owns high conductivity [17]. In recent years, RGO based composites have been used for various applications including biosensor [18], solar cells [19] and super capacitors [20].

Graphene-based metal oxide (RGO-MO) nanocomposites consist of the highly conductive carbon film serving as an anchor for the metal oxide nanocrystals and are emerging as a class of new exciting materials [21]. There are several reports on the synthesis of graphene-metal oxide nanocomposites using techniques such as ultrasonic spray pyrolysis [22], hydrothermal [23], solvothermal [24] and microwave-assisted reduction [25].

Among various metal oxides, zinc oxide (ZnO) is an exceptional material with high specific surface area, nontoxicity, chemical stability, electrochemical activity and the high electron mobility of ~115−155 cm^{-2} V^{-1} s^{-1}(band gap energy - 3.37 eV) [26,27]. Zinc oxide is also one of the well-studied transition metal oxides in electrochemistry. Some studies demonstrated that decoration of ZnO nanoparticles on graphene sheets could enhance the electrocatalytic activity of the composite. Nayak et al. demonstrated a high-performance electrochemical dopamine sensor based on the ZnO/grapheme nanocomposite [28]. Jiang et al. and Lp-Fu et al.reported graphene–ZnO nanocomposites for ultrasensitive electrochemical sensing of acetaminophen and

phenacetin [29] and of uric acid [30] respectively. Recently many electrochemical sensing works based on Graphene composites for the detection of pesticides are reported. Graphene - chitosan composite [31], Graphene/gadolinium Prussian Blue analogue nanocomposite composite [32] , Nano-TiO2/graphene composite [33] and Silver /Graphene nanoribbon composite [34] have been applied as enzymeless sensor for detection of Methyl parathion. Moreover, the graphene oxide (GO) and reduced of graphene oxide (RGO) also used to fabricate the composites used in sensor studies such as Electrochemically reduced graphene (ERGO) [35], ERGO/naffion [36], Cobalt Porphyrin- Co_3O_4-GO nanocomposite [37], GO /Chitosan [38], CeO_2/RGO nanocomposite [39] and GO/MWCNT [40].Interestingly Graphene quantum dots, a multifunctional composite also employed for Pesticide Detection [41]. In the present work, RGO-ZnO nanocomposite is prepared via a simple hydrothermal method. The RGO-ZnO nano composite modified electrode is used as an electrochemical sensor for the detection of Methyl parathion.

II. Experiments

2.1. Materials and reagents

Zinc nitrate hexahydrate $Zn(NO_3)_2.6H_2O$, hydrazine aqueous solution (25%) and grapheme oxide powder were purchased from Sigma-Aldrich. All other chemicals used were analytical-grade reagents without further purification. Phosphate buffer solution (PBS) was prepared by mixing 0.1M KH_2PO_4 and K_2HPO_4 solution to appropriate pH.Milli-Q water was used throughout the experiments.

2.2.1 Synthesis of nano ZnO particles

An aqueous solution (0.5 mol/L) of zinc nitrate hexahydrate ($Zn(NO_3)_2.6H_2O$) was mixed with the appropriate amount of 1 mol/L NaOH solution under continuous stirring and the mixture was put into a Teflon-lined-stainless steel autoclave unit for hydrothermal reaction at 150 ˚C for 7h., the reactor was naturally cooled to room temperature. The product obtained after hydrothermal reaction was filtered, washed with de-ionized water till the pH of the final solution was 7.0. Finally the as-prepared sample was calcined at 600˚ C in a muffle furnace for 1 hr.

2.2.2 Synthesis of RGO

GO (1 mg ml^{-1}) was suspended in 2 ml of hydrazine (5wt%) aqueous solution and the solution was sonicated for 1h and then transferred to a 30 mL stainless steel autoclave (Teflon lined) and heated at 150˚C for 2h. The sample obtained was centrifuged and dried.

2.2.3 Synthesis of RGO–ZnO composite

Hydrothermal method is adopted for synthesis of RGO-ZnO composite. The various steps involved in the method is described as follows: In the first step, 10 mg of GO was suspended in 10mL of water and the suspension was sonicated for 2h to prepare GO dispersion. To the GO dispersion, 10mL of $Zn(NO_3)_2$ was gradually added under stirring. Then 2mL hydrazine solution (5wt %) was added into the mixture. The gray colored slurry formed after 1 h sonication was transferred to a 30 mL stainless steel autoclave (Teflon lined) and heated at 120 ◦C for 2h.The sample obtained was centrifuged and dried in an oven at 70^{o}C to produce RGO–ZnO composite.

2.3 Characterization

Fourier transform infrared analysis (FTIR) was carried out using Nicolet iS5 (Thermo Scientific) in transmission mode in the wave number range of 400–4000 cm^{-1}. Surface morphology of samples were analyzed by scanning electron microscope (SEMCarl Zeiss,EVO 18,Germany) and elemental mapping studies made by Energy Dispersive X-ray Spectrometer Bruker (X Flash 6130).Atomic force microscopy(AFM) studies were performed by multimode AFM with Nanosurf Easyscan2 controller (Switzerland)in tapping mode.HR-TEM (Technai G2 F30) was performed at an accelerating voltage of 300 kV. For electrochemical investigation, a GCE was polished with alumina-water slurry followed by rinsing with water. For the electrode surface modification, 1μL of composite dispersion (1mg/mL) was dropped onto the GCE surface and dried at room temperature. Electrochemical measurements were performed on a CH Instruments 650C Electrochemical Workstation (CHI-650C,CH Instruments, Texas, USA) using a three electrode system. A platinum wire was used as the auxiliary electrode and an Ag/AgCl as the reference electrode.

III. Results and Discussion

3.1 Characterization of synthesised RGO–ZnOnanocomposite

3.1.1 FT-IR spectral Analysis

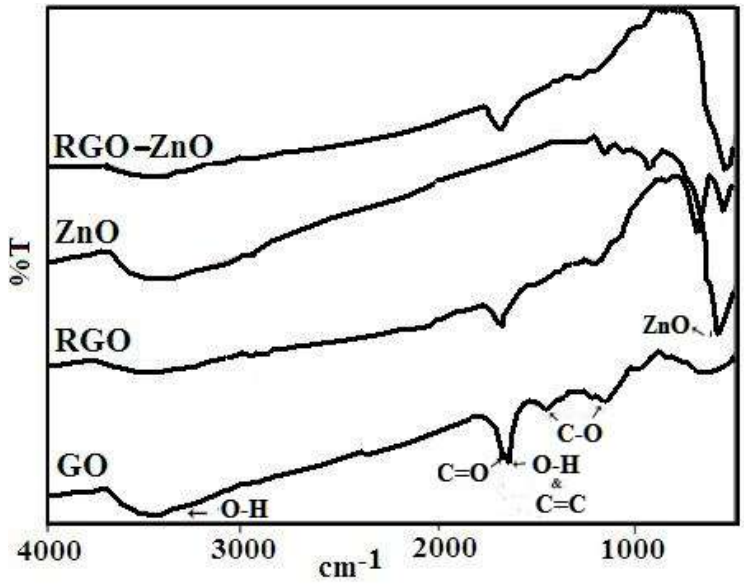

Fig. 1.FTIR spectra of GO, RGO, pure ZnO and RGO–ZnO composite

The prepared RGO-ZnO nanocomposite was characterized using FT-IR spectroscopy and shown in Fig. 1.The reduction of oxygen containing functional groups in the GO after the thermal treatment was confirmed by FT-IR analysis. The spectrum of GO exhibits the bands corresponds to OH stretching vibration (3400 cm^{-1}), O-H bending vibration (1621 cm^{-1}), C=O stretching vibration (1726 cm^{-1}), C-O stretching vibrations of epoxy group(1240 cm^{-1}), C-OH stretching vibrations(1380 cm^{-1}) and C=C skeletal ring vibrations (1627) of the graphene oxide. But, a drastic decrease in intensity of these bands is observed in both the pure RGO and RGO-ZnO composite after hydrothermal reduction. The spectrum of pure ZnO shows a band at 470 cm^{-1} corresponding to the Zn-O stretching vibration. Due to interactions between the ZnO and residual epoxy and hydroxyl functional groups of the RGO, the band of ZnO was red-shifted to 440 cm^{-1} in the RGO-ZnO nanocomposite.

3.1.2 Morphological characterization using SEM-EDX, HR-TEM and AFM

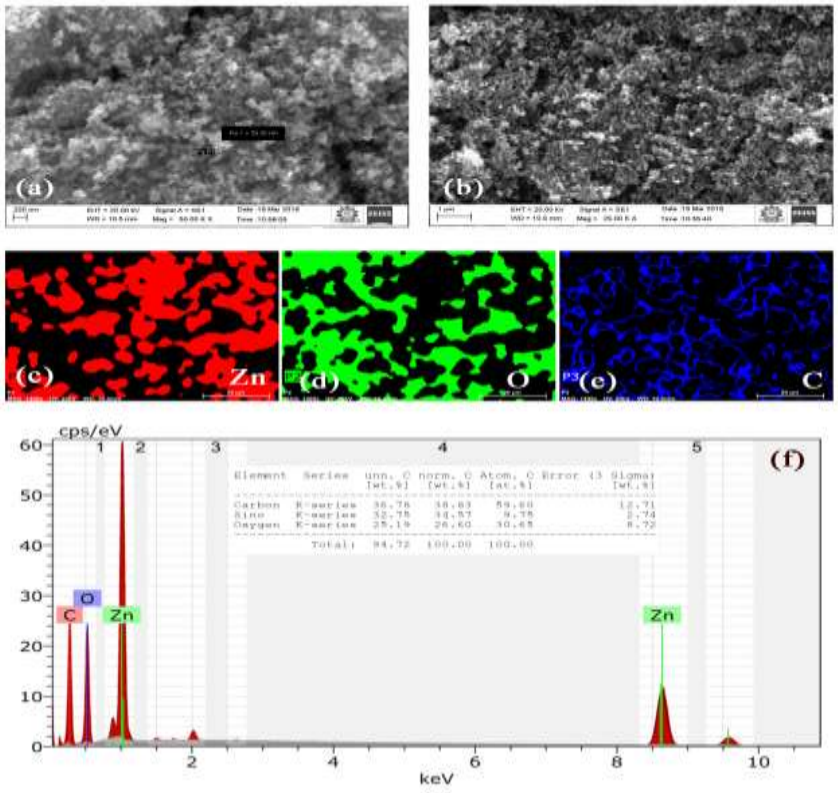

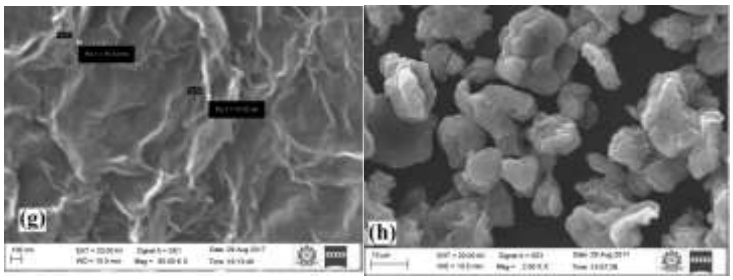

Fig. 2. SEM images of RGO-ZnO composite at different magnification (a-b) and elemental mapping (c-e) with edax spectrum (f) SEM images of (g) RGO and (h) ZnO

The SEM image in Figs. 2(a-b) provides the morphology of RGO-ZnO composite. The uniformly grown ZnO nanoparticles were closely affixed onto the surface of RGO sheets. Due to the remaining oxygen-containing groups in RGO, the electrostatic attraction between the positively charged Zn^{2+} and the negatively charged precursors in the GO sheets play a crucial role in the firm attachment of the ZnO NPs on RGO in the final product. The EDS result in Figs. 2(f) and corresponding elemental mapping in Figs. 2(c-e) confirm the presence of Zn, O and C in the composites. The SEM image of RGO in Fig. 2(g) shows that the RGO nanosheets are wrinkled and their size is found to be about 16.72 nm. The SEM of ZnO in Fig.2 (h) shows the size ZnO NPs is 20nm.

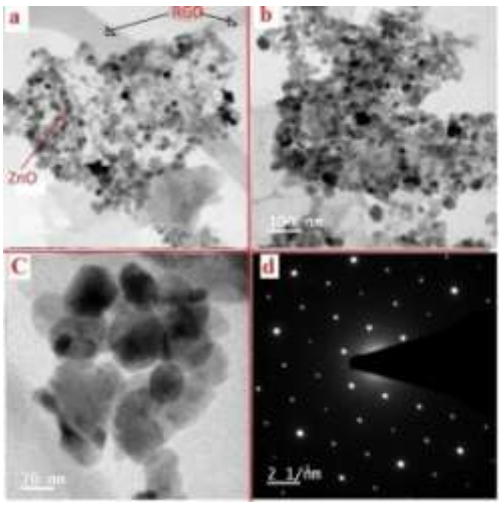

Fig.3.HRTEM images of RGO-ZnO composite (a-c) and SAED Pattern (d)

High resolution TEM was performed to determine the physical nature of ZnO in the composite more clearly. Fig. 3 depicts the HR-TEM images of RGO-ZnO composite. Fig 4a &4b revealed that the ZnO NPs were dispersed densely on the RGO sheets. In some regions, aggregation of ZnO NPs was occurred on the surfaces of RGO nano sheets, and most of the NPs were found on the nano sheets. Fig. 4c revealed the NPs to be 5-10 nm in size. Selected area electron diffraction (SAED) shows in Fig.4d indicate crystalline nature of the composite. The SAED pattern consisted of four diffraction rings counting from the center, the 1st, 2nd, 3rd, and 4th rings were assigned to the (100), (101), (102) and (211) planes, respectively. The SAED pattern also confirmed the wurtzite structure of ZnO.

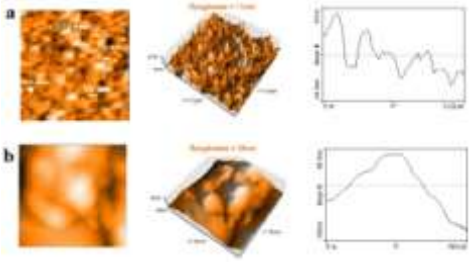

Fig.4a) 2D and 3D AFM images of GO with Height profile b) 2D and 3D AFM images of RGO –ZnO composite with Height profile parathion

The surface morphology is further investigated by AFM studies. Higher roughness value of RGO-ZnO as shown in Fig. 4 than GO again confirms the composite formation and its better adsorption nature.

3.1.3 Electrochemical Studies

3.1.3.1 Electrochemical behavior of MP on the RGO-ZnO modified electrode

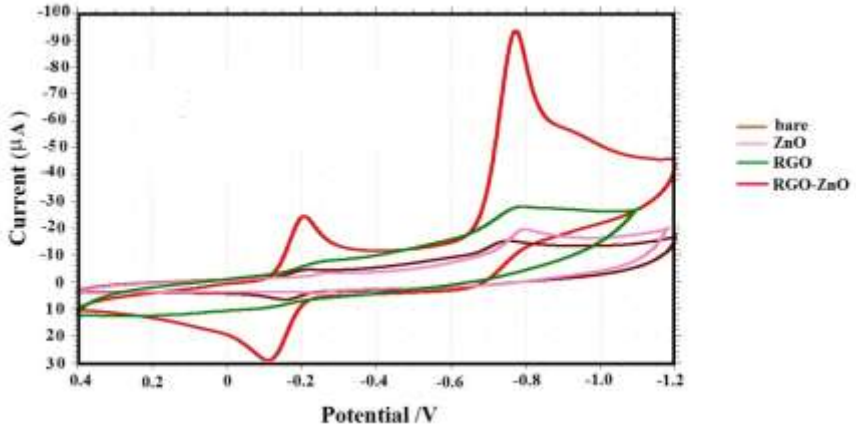

Fig. 5. Cyclic voltammograms of bare, ZnO, RGO and RGO–ZnO modified GCE in 0.1M PBS of P^H=7 containing 1mM Methyl parathion. Scan rate: 50mV/s

The prepared RGO-ZnO nanocomposite was coated on GCE and its sensing nature for methyl parathion was investigated. As shown in Fig. 4, obvious clear redox peaks could be observed on the bare GCE, ZnO, RGO and RGO–ZnO-modified GCEs with current response as -15.2,-20.3,-28.0 and -93.2 μA respectively. The increase in peak current of RGO–ZnO modified GCE represents its significant electrocatalytic activity toward MP detection compared to bare GCE, ZnO and RGO modified GCEs.

A sharp irreversible reduction peak appeared at 0.793V is due to the four-electron reduction of the nitro group (–NO_2) to hydroxylamine as shown in reaction (1) of Scheme 1 during the first cathodic scan. The peak observed at -0.077V during the anodic scan represents the oxidation (–NHOH) to the nitroso (–NO) group as shown in reaction (2) of scheme 1. Another reduction peak appeared at -0.215V results from the reversible reduction of nitrso group to hydroxylamine during the successive cycles as shown reaction (3) of Scheme 1. From the various reports of aromatic nitro compounds, it is inferred that only two electron involved in reversible redox process (reaction 2 &3) as given in Scheme 1.

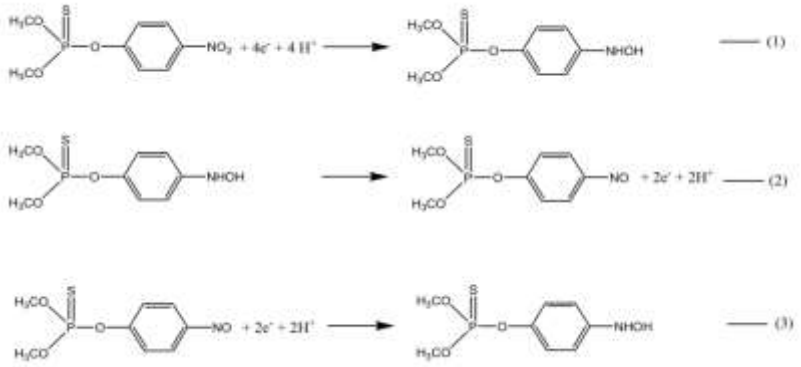

Scheme 1

Fascinatingly,, the oxidation peak current of methyl parathion at RGO-ZnO modified GCE is 3.5 fold higher than that of RGO modified GCE and 4.8 fold higher than ZnO modified GCE.

3.1.3.2 Effect of Scan Rate

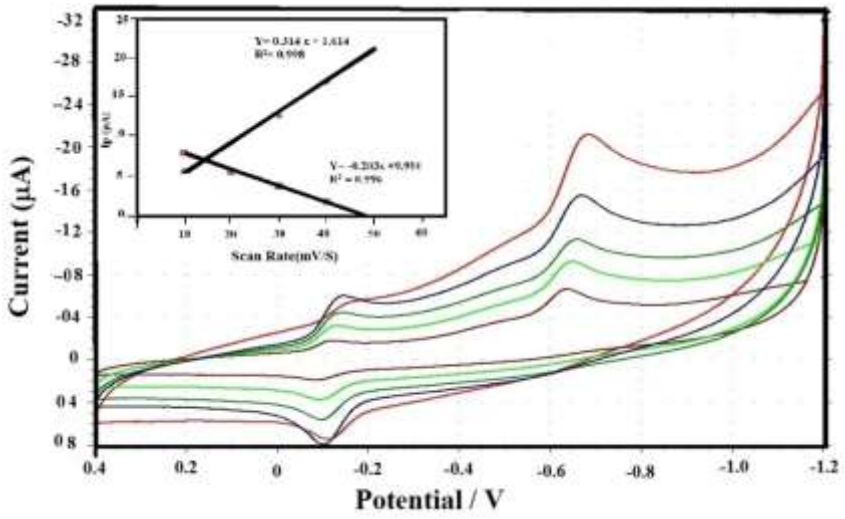

Fig. 6. Cyclic voltammograms of the RGO–ZnO-modified GCE at scan rate of 10-50 mVs^{-1} in 0.1MPBS containing 1mM MP. Inset shows the linear dependence of Ipa (■) and Ipc(■) on scan rate (10 to 50 mV s−1).

The influence of scan rate (*v*) on the redox peak current of MP at RGO-ZnO/GCE electrode was investigated (Fig. 5). Both the anodic and cathodic peak currents of MP are linearly proportional to scan rates in the range of 10~50mVs^{-1}, confirming that the electrode reaction of MP at RGO-ZnO/GCE is an adsorption control process. The linear regression equation for cathodic and anodic peak currents are obtained as represented in Eqs (1) and (2), respectively

$$I_{pc} = 0.381\ x + 1.674\ (R^2 = 0.998)\ \text{----------(1)}$$

$$I_{pa} = -0.203x + 9.910\ (R^2 = 0.996)\ \text{----------(2)}$$

Where *I*pc is the cathodic peak current and *I*pa is the anodic peak current. The *v* stands for the scanning rate in the unit of mV s^{-1} and R^2 is a regression coefficient.

3.1.3.2 Square Wave Voltammetry (SWV)

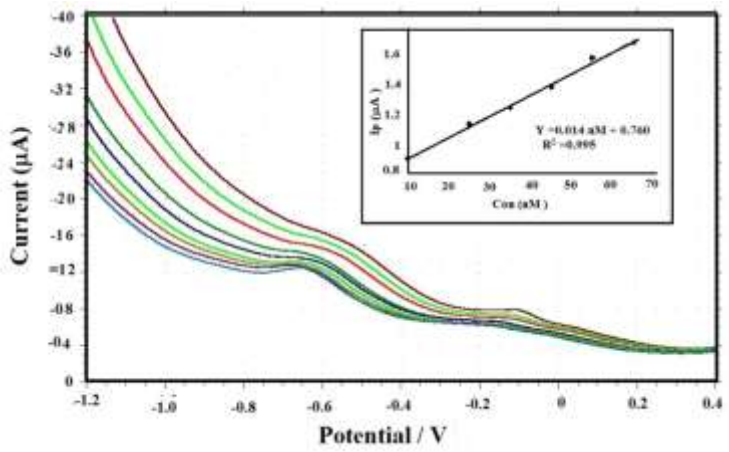

Fig.7. Square wave voltammograms of increasing methyl parathion concentrationin 0.1M PBS (pH 7.0) at RGO-ZnO/GCE, from bottom to top, with concentrations of0, 5, 10,15, 25,35, 45, 55,65, 75, 85 nM, respectively. The inset shows the calibration curve.

Fig. 7 depicts the well-defined SWV peaks correspond to different concentration of methyl parathion at RGO-ZnO/GCE. A linear relationship between the reduction peak current and the methyl parathion concentration is obtained over the concentration range from $5x10^{-9}$ to $85x10^{-9}$ M. The linear regression equation was obtained as Ip (µA) = 0.014nM + 0.76, with a correlation coefficient of 0.995 and a detection limit of 1.22×10^{-9}M which was calculated from the signal-to-noise ratio of 3.

Table 1. Comparison of analytical results of previously reported electrochemical sensor studies of MP based on Graphene modified electrode with RGO-ZnO modified electrode

S.No	Electrode	Medium	Method	Linear range / M	Detection limit / M	Ref.
1	Graphene-chitosan	ABS, pH 5.2	SWV	0.02- 1.5 x 10^{-9}	3.00 x10^{-9}	31
2	Electrochemically RGO	PBS , pH 7	SWV	3.0 x 10^{-10} – 2 x10^{-9}	8.87 x 10^{-10}	35
3	Graphene / GPBA	PBS , pH 7	DPV	0.008 -10 x10^{-6}	1.00 x10^{-9}	32
4	NanoTiO_2 / Graphene	ABS, pH 5.2	LSV	5~100 x 10^{-6}	1.00 x10^{-9}	33
5	Cobalt Porphyrin/ Co_3O_4/GO	PBS , pH 7	DPV	4.0×10^{-7} to 2.0×10^{-5}	1.10 x10^{-8}	37
6	RGO / Cobalt Bipyridyl	PBS , pH 7	Amperometry	0.05-1700 x10^{-6}	2.90 x10^{-9}	34
7	ZnO/RGO	PBS , pH 7	SWA	5-100 x10^{-9}	1.22 x 10^{-9}	Present work

.

GPBA: Gadolinium Prussian Blue analogue, SWV: Square wave voltammetry DPV: Differential pulse voltammetry; PBS: Phosphate buffer solution, ABS: Acetate buffer solution. LSV: Linear sweep voltammetry.

The results of various electrochemical sensor works based on graphene modified electrodes are compiled and compared with that of the present work in Table 1. The detection limit of the present work is comparable [32, 33,37 and 35] or even better than [31, 34] the other reported values.

3.1.3.3 Electrochemical impedance spectrum (EIS)

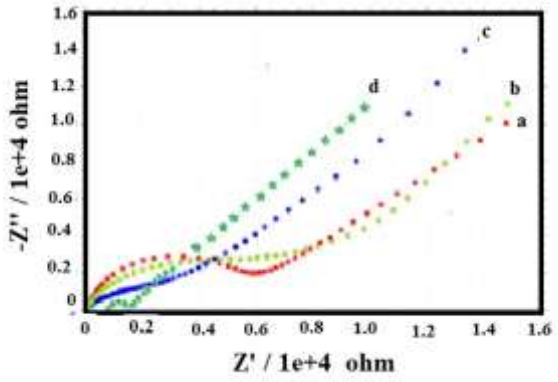

Fig.8. Electrochemical impedance spectra of the bare GCE (a), ZnO/GCE (b), RGO/ GCE (c) and RGO-ZnO/GCE (d) in 0.1 M KCl containing 3mM $[Fe(CN)6]^{3-/4-}$.

Electrochemical impedance spectrum was obtained by studying the performance of the electrode interface. Fig. 8 shows the electrochemical impedance spectra of the bare GCE (a), ZnO/GCE (b), RGO/ GCE (c) and RGO-ZnO/GCE (d) in 0.1M KCl containing equimolar $[Fe(CN)_6]^{3-/4-}$. As shown, the electrode RGO-ZnO/GCE has comparatively low electron transfer resistance. Moreover, the Nyquist plot of RGO-ZnO/GCE is almost straight line which represents that the RGO-ZnO/GCE still keeps fast electron transfer.

3.2 Real Sample Analysis

The real sample analysis has been carried out to evaluate the application proposed method by using vegetable samples. Ether solvent was used for extracting MP from the two vegetable (carrot) samples (5 g each) spiked with standard MP solutions (25 x 10^{-9} M and 35 x 10^{-9} M) concentration of MP for about 24 h and the collected extracts were filtered through a 0.45µm membrane and then evaporated to dryness. The solution of sample was prepared by dissolving the residue in 0.1M PSB (pH 7) and made upto 100mL. The SWV peaks obtained for the sample were compared with that obtained for the standard MP solutions. The SWV profiles and the peak potentials compare very well with those obtained for the standard MP solutions. By substituting SWV current corresponds two carrot samples in the calibration equation, Ip (µA) = 0.014nM +

0.76, the amount of MP found in the samples is estimated. From the % recovery data (Table 2) ,it is deduced that nearly 90% recovery is possible.

Table 2.Sensing of MP present in carrot sample at RGO-ZnO/ GCE.

Sample	Added/nM	Detected/nM	Recovery %
1	25	23	92
2	35	32	91

3.3 Interference studies

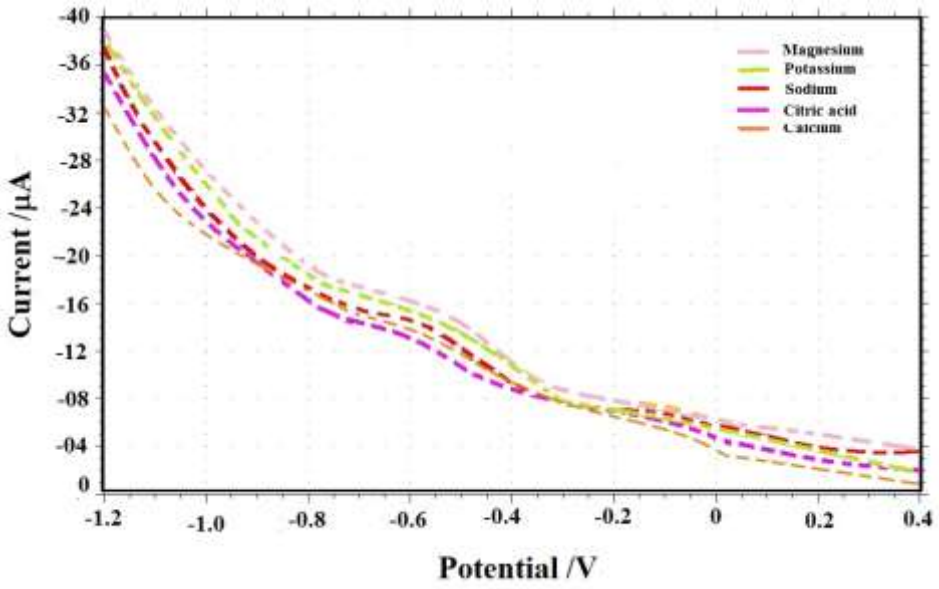

Fig.9. SWA response for Interference study of 25 nM MP with 6 different compounds: Potassium, Sodium, Calcium, Magnesium Citric acid and Glucose.

SWV analysis carried out at RGO-ZnO/GCE in the presence of a few foreign substances such as Sodium, Potassium, Magnesium, Calcium and Citric acid which are rich in biological sample and supposed to have interferences on reduction peak current of MP. 200-fold $CaCl_2$, $MgCl_2$, NaCl, KCl, 100-fold glucose and citric acid were added to 25 nM MP. As shown in Fig.9, no considerable change of the SWA cathodic peak current of MP in the presence of interferents was observed. Moreover, the ratio (%) between the reduction peak current of MP in the presence and absence of the interferences is found in the range of 95% to 105%, which further confirms that the interferences have almost no influence on the reduction peak current at the surface of the sensor. It proves the efficient sensing nature of RGO- ZnO/GCE and hence it can be recognized as a good electrochemical sensor.

IV. Conclusion

A simple one-pot hydrothermal method was adopted to prepare RGO–ZnO nanocomposite. The results of the electrochemical sensing method proved the efficient sensitivity and selectivity of RGO–ZnO nanocomposite-modified GCE towards the determination of MP. Lower detection limit and a wide detection range with fast response shown by the method enhances and also evidences the validity of the proposed method. An excellent performance of the fabricated sensor in anti-interference studies indicates its promising nature to trace out MP in real samples.

Acknowledgement

The author gratefully thanks University Grand Commission, New Delhi and the Secretary, the Principal and the Head of Chemistry Department, V.O.Chidambaram College, Thoothukudi, Tamil Nadu, India to carry out this research work.

References

[1] M.E. Leon-Gonzalez and A.Townshend, Flow-injection determination of paraoxon by inhibition of immobilized acetolinesterase, Anal Chim Acta, 236(2), 1990, 267-272.

[2] A.Mulchandani, W Chen, P.Mulchandani, J.Wang, and K.R.Rogers, Biosensors for direct determination of organophosphate pesticides. Biosens Bioelectron, 16(4-5), 2001, 225-30.

[3] D.B Barr, J.R. Barr, V.L Maggio, R.D Jr Whitehead, M.A.Sadowski, R.M. Whyatt, and L.L.Needhamm, A multi-analyte method for the quantification of contemporary pesticides in human serum and plasma using high- resolution mass spectrometry, J Chromatogr B, 778(1-2), 2002, 99-111.

[4] A.Cappielo, G Famiglini, P.Palma and F.Mangani, Trace Level determination of new organo- phosphorous pesticides in water with direct electron ionization LC/MC, Anal Chem., 74 (14), 2002,3547-3554.

[5] S. Lacorte and D.Barcelo, Determination of parts per trillion levels of organophosphorus pesticides in ground water by automated on-line liquid-solid extraction followed by liquid chromatography/ atmospheric pressure chemical ionization mass spectrometry using positive and negative ion modes of operation, Anal Chem., 68(15), 1996, 2464-2470.

[6] D.Barcelo and M.C.Hennion, Sampling of polar pestcides from water matrices,Anal Chim Acta, 338(3-18), 1997, 3-18.

[7] G.A.Evtugyn, H.C.Budnikov and E.B.Nikolskaya, Sensitivity and selectivity of electrochemical enzyme sensors for inhibitor determination,. Talanta, 469(4), 1998, 465-484.

[8] V.A.Pedrosa, J.Caetano, S.A.S Machado, R.S.Freire and M.Bertotti, Acetylcholinesterase immobilization on 3- mercaptopropionic acid self assembled monolayer for determination of pesticides, Electroanalysis, 19(13), 2007,1415-1420.

[9] M.Priti, M Ashok, K.Irina and W. Chen, Biosensor for direct determination of organophosphate nerve agents. 1. Potentiometric enzyme electrode, Biosens Bioelectron, 14(1), 1999, 77-85.

[10] M.J,Schoning, R.Krause, K.Block, M.Musahmeh and J.Wang, A dual amperometric/ Potentiometric FIA-based biosensor for the distinctive detection of organophosphorus pesticides, Sens.Actuat. B, 95(1-3), 2003,291-296.

[11] C.G.Tsiafoulis and C.G. Nanos, Determination of azinphos-methyl and parathion-methyl in honey by stripping voltammetry, Electrochim.Acta, 56(1) , 2010,566-574.

[12] X.Tan, B. Li and C.Liew and C.Li, Electrochemical fabrication of molecularly imprinted porous silicate film electrode for fast and selective response of methyl parathion, Biosens Bioelectron, 26(2) , 2010, 868 -871.

[13] L. Zhang, Y.Li, L.Zhang and D.W.Li, D.Karpuzov and Y.T.Long, Electrocatalytic Oxidation of NADH on Graphene Oxide and Reduced Graphene Oxide Modified Screen-Printed Electrode, Int. J. Electrochem. Sci., 6 (3), 2011,819– 829.

[14] P. Selvakumar, A.T. Ezhil Vilian, Shen-Ming Chen, Direct Electrochemistry of Glucose Oxidase at Reduced Graphene Oxide/Zinc Oxide Composite Modified Electrode for Glucose Sensor, Int.J. Electrochem. Sci, 7(3) , 2012,768 – 784.

[15] S. Stankovich, D.A.Dikin, R.D.Piner, K.A.Kohlhaas, A.Kleinhammes, Y. Jia, Y Wu, S.B.T.Nguyen and R.S.Ruo, Synthesis of graphene-based nanosheets via chemical reduction of exfoliated graphite oxide,Carbon, 45(7),2007, 1558–1565.

[16] Y. Shao, J.Wang, H.Wu, J.Liu, I.A.Aksay and Y.Lin, Electrochemical Performance of Graphene as Effected by Electrode Porosity and Graphene functionalization, Electroanalysis, 22(10) , 2010, 1027 – 1036.

[17] M.D.Stoller, S.Park, Y.Zhu, J.An and R.S.Ruoff, Graphene-Based Ultracapacitors, Nano Lett, 8 (10), 2008, 3498–3502

[18] Z.Wang, X.Zhou, J.Zhang, F.Boey and H.Zhang, Direct Electrochemical Reduction of Single-Layer Graphene Oxide and Subsequent Fictionalization with Glucose Oxidase.J. Phys. Chem. C**,** 113(32), 2009, 14071–14075.

[19] V.K.Rana, M.C.Choi, J.Y.Kong, G. Y.Kim, M.J.Kim, S.H. Kim, S.Mishra, R.P. Singh and C.S.Ha, 2D-Aligned Graphene Sheets in Transparent Polyimide/Graphene Nanocomposite Films Based on Noncovalent Interactions Between Poly(amic acid) and Graphene Carboxylic Acid, Macromol. Mater. Eng, 296(2) , 2011,131–140.

[20] X.Wang, L. Zhi and K.Mullen, Transparent, Conductive grapheme electrode for dye- sensitized solor cells, Nano Lett, 8(1) ,2008, 323-327.

[21] T.Ramanathan, A.A Abdala, S.Stankovich, D.A.Dikin, M.Herrea-Alonso and R.D. Piner, Functionalized graphene sheets for polymer nanocomposites, Nat Nanotechnol, 3(1) , 2008 , 327–31.

[22] T. Lu, Y.Zhang, H.Li, L.Pan, Y Li and Z.Sun, Electrochemical behaviours of graphene-ZnO and graphene-SnO_2 composite films for supercapacitors, Electrochim.Acta, 55(13) , 2010,4170–4173.

[23] Y.J. Kim, Hardiyawarman, A.Yoon, M.Y.Kim, G.C.Yi and C.L.Liu, Hydrothermally grown ZnO nanostructures on few-layer graphene sheets, Nanotechnology,22(27) , 2011,245603–222011.

[24] J. Wu, X.Shen, L.Jiang, K.Wang and K.Chen, Solvothermal synthesis and characterization of sandwich-like graphene/ZnO nanocomposites, Appl Surf Sci, 256 (9), 2010, 2826–2830.

[25] T.Lu, L.Pan, H.Li, G.Zhu, T.Lv and X.Liu, Microwave-assisted synthesis of graphene–ZnO nanocomposite for electrochemical supercapacitors, J Alloys Compd, 509(18) , 2011,5488–5492.

[26] X. W.Sun and H. S. Kwok, Optical properties of epitaxially grown zinc oxide films on sapphire by pulsed laser deposition, J. Appl. Phys, 86(1), 1999,408-411.

[27] P.Selvakumar, A.T. Ezhil Vilian and S.M. Chen, Direct Electrochemistry of Glucose Oxidase at Reduced Graphene Oxide/Zinc Oxide Composite Modified Electrode for Glucose Sensor, Int. J. Electrochem. Sci., 7(3), 2012**,** 2153 – 2163.

[28] P.Nayak, P.N. Santhosh and S.Ramaprabhu, Electrochemical sensor for dopamine based on ZnO decorated grapheme nanosheets as the transducer matrix, Graphene. 1(1) , 2013,25–30.

[29] L.Jiang, S.Gu, Y. Ding, F.Jiang and Z.Zhang, Facile and novel electrochemical preparation of a graphene-transition metal oxide nanocomposite for ultrasensitive electrochemical sensing of acetaminophen and phenacetin, Nanoscale, 6(1), 2014, 207–214.

[30] L.Fu, Y.Zheng, A.Wang, Wen Cai, B.Deng and Zhi Zhang, An Electrochemical Sensor Based on Reduced Graphene Oxide and ZnO Nanorods-Modified Glassy Carbon Electrode for Uric Acid Detection, Arab J Sci Eng, 41(1) , 2016, 135–141.

[31] S**.** Yang , S. Luo , C. Liu and .Wei , Direct synthesis of graphene–chitosan composite and its application as an enzymeless methyl parathion sensor**,** Colloids Surf B Biointerfaces., 96 ,2012, 75-79.

[32] Yuqin Li, Minrong Xu, Peipei Li, Jing Dong and Shiyun Ai, Nonenzymatic sensing of methyl parathion based on graphene/gadolinium Prussian Blue analogue nanocomposite modified glassy carbon electrode, Anal Methods.,6(7), 2014, 2157-2162.

[33] B. Song, W. Cao and Y.Wang, A methyl parathion electrochemical sensor based on Nano-TiO_2, graphene composite film modified electrode, FULLER NANOTUB CAR N., 24(7), 2016,435-440.

[34] Mani Govindasamy, Subramanian Sakthinathan, Shen-Ming Chen, Te-Wei Chiu, Anandaraj Sathiyan and Johnson Princy Merlin, Reduced Graphene Oxide Supported Cobalt Bipyridyl Complex for Sensitive Detection of Methyl Parathion in Fruits and Vegetables, Electroanalysis., 29(8),2017, 1950-1960.

[35] Tharini Jeyapragasam, R.Saraswathi, Shen-Ming Chen1 and Bih-Show Lou , Detection of Methyl Parathion at an Electrochemically Reduced Graphene Oxide (ERGO) Modified Electrode, Int.J. Electrochem. Sci., 8(9), 2013, 12353-12366.

[36] ShuoWu , F.Huang, X.Lan, J.Wang, X.Wang and C.Meng, Electrochemically reduced graphene oxide and Nafion nanocomposite for ultralow potential detection of organophosphate pesticide, Sens. Actuat. B, 177 (1),2013, 724-729.

[37] F.Liu, Y.Du, Y.Cheng, W. Yin, C.Hou , D.Huo, Can Chen and H. Fa, A selective and sensitive sensor based on highly dispersed cobalt porphyrin-Co_3O_4-graphene oxide nanocomposites for the detection of methyl parathion, J Solid State Electrochem,20(3) ,2016, 599-607.

[38] P.Reddy Prasad , A.E.Ofamaja , C.Nageswara Reddy and E.B.Naidoo, Square Wave Voltammetric Detection of Dimethylvinphos and Naftalofos in Food and Environmental Samples Using RGO/CS modified Glassy Carbon Electrode, Int. J. Electrochem. Sci., 11(12) ,2016, 65-79.

[39] Ali A. Ensafi, Rasool Noroozi, Navid Zandi–-Atashbar and B. Rezaei, Cerium(IV) oxide decorated on reduced graphene oxide, a selective and sensitive electrochemical sensor for fenitrothion determination, Sens. Actuat, B,245,2017, 980-987.

[40] R. Devasenathipathy, K. Kohila rani and S.Wang, Fabrication of Graphene Oxide-MWCNTs Nanocomposite Modified Glassy Carbon Electrode for the Sensitive Determination of Amitrole, Int. J. Electrochem. Sci., 12 (6), 2017, 5888-5897.

[41] Erhan Zor, Eden Morales-Narváez, Alejandro Zamora-Gálvez, Haluk Bingol, Mustafa Ersoz, and Arben Merkoçi, Graphene Quantum Dots-based Photoluminescent Sensor: A ultifunctional Composite for Pesticide Detection, ACS Appl. Mater. Interfaces, 7(36) , 2015, 20272-20279.

IOSR Journal of Applied Chemistry (IOSR-JAC) is UGC approved Journal with Sl. No. 4031, Journal no. 44190.

S. Muthumariappan. "Nonenzymatic Sensing Of Methyl Parathion Based On RGO-Zno Nanocomposite Modified Glassy Carbon Electrode." IOSR Journal of Applied Chemistry (IOSR-JAC) , vol. 10, no. 9, 2017, pp. 55–64.